Artificial Evolution for 3D PET Reconstruction

Franck P. Vidal[1,2,⋆], Delphine Lazaro-Ponthus[2], Samuel Legoupil[2], Jean Louchet[1,3], Évelyne Lutton[1], and Jean-Marie Rocchisani[1,4]

[1] INRIA Saclay - Île-de-France/APIS, Parc Orsay Université, 4 rue Jacques Monod 91893 Orsay Cedex, France,
[2] CEA, LIST, Saclay, F-91191 Gif-sur-Yvette, France
[3] Artenia, 24 rue Gay-Lussac, 92320 Châtillon, France
[4] Paris XIII University, UFR SMBH & Avicenne hospital, 74 rue Marcel Cachin, 930013 Bobigny, France

Abstract. This paper presents a method to take advantage of artificial evolution in positron emission tomography reconstruction. This imaging technique produces datasets that correspond to the concentration of positron emitters through the patient. Fully 3D tomographic reconstruction requires high computing power and leads to many challenges. Our aim is to reduce the computing cost and produce datasets while retaining the required quality. Our method is based on a coevolution strategy (also called Parisian evolution) named "fly algorithm". Each fly represents a point of the space and acts as a positron emitter. The final population of flies corresponds to the reconstructed data. Using "marginal evaluation", the fly's fitness is the positive or negative contribution of this fly to the performance of the population. This is also used to skip the relatively costly step of selection and simplify the evolutionary algorithm.

1 Introduction

Fully 3D tomographic reconstruction in nuclear medicine requires high computing power and leads to many challenges. However the use of evolutionary computation in this field has been largely overlooked.

Conventional reconstruction methods are analytical or based on statistical analysis, such as the maximum-likelihood expectation-maximization (ML-EM)[1] [1] or the ordered subset expectation-maximization (OS-EM) [2] algorithms. A broad overview of reconstruction algorithms in nuclear medicine can be found in [3]. The trend today is to use more general methods that can integrate more realistic models (application-specific physics and data acquisition system geometry). To date, the use of such methods is still restricted due to the heavy computing power needed.

Evolutionary algorithms have proven to be efficient optimisation techniques in various domains [4], including medicine [5] and medical imagery [6–8]. In a previous paper, we showed that a cooperative coevolution strategy (also called

⋆ member of Fondation Digiteo (http://www.digiteo.fr).
[1] See Section on "Acronyms" for a list of acronyms.

Parisian evolution) called "fly algorithm" [9] could be used in single-photon emission computed tomography (SPECT) reconstruction [10].

However, positron emission tomography (PET) – the other main tomographic technique in nuclear medicine – has taken over SPECT in routine clinical practice. Although the underlying physics and the design of imaging systems in SPECT and PET are different, it is possible to use a reconstruction method that is similar to the one that we initially proposed for SPECT data. In this case, PET raw data needs to be converted into sinograms (see Fig. 4(b) for an example of synthetic sinogram). This pre-processing step introduces sampling that constrains the resolution of the reconstructed images and most of the input sinogram is empty. During the reconstruction using the evolutionary algorithm, it is difficult to take into account physics and the geometrical properties of the imaging system due to this intermediate data representation, and also only a few pixels of the simulated images will contain useful information. Moreover, the issue regarding the memory usage that has been identified in [10] remains. This is therefore not straightforward to achieve an efficient fully 3D reconstruction in PET and we propose in this paper a new approach to overtake the disadvantages presented above. It makes use of a simplified geometry model that still matches the acquisition system properties. Our long term goal is to include Compton scattering (the dominant physical perturbation in the input data) correction in the evolution loop to further improve the quality of the final reconstructed image.

The following section gives an overview of the context and objective of this study. Our methodology is described in Section 3. The results and performance of our reconstruction method is presented in Section 4. The last section discusses the work that has been carried out and it provides directions for further work.

2 Context and Objectives

Nuclear medicine [11] appeared in the 1950's. Its principle is to diagnose or treat a disease by administering to patients a radioactive substance (also called tracer) that is absorbed by tissue in proportion to some physiological process. This is the radiolabelling process. In the case of diagnostic studies, the distribution of the substance in the body is then imaged. It is generally a functional form of imaging because the purpose is to obtain information about physiological processes rather than anatomical forms and structures. When a pathology occurs, the metabolism increases and there are more tracer molecules in the pathology area. Consequently, the radioactivity also increases.

There are two classes of techniques to produce 3D data in nuclear medicine: SPECT and PET. They allows 3D reconstruction of the distribution of the tracer through the body. In SPECT, a gamma emitter is used as radioactive tracer. Similarly to conventional computed tomography (CT) [12], multiple 2D projections are recorded at successive angles. It is followed by a mathematical reconstruction. The main limitations include the finite spatial resolution and the sensitivity of detectors, physical effects (such as absorption, Compton scattering,

and noise), long exposure times, and accuracy of the reconstruction. In PET, a positron emitter is used as radionuclide for labeling rather than a gamma emitter. After interactions, a positron combines with an electron to form a positronium, then the electron and positron pair is converted into radiations: this is the annihilation reaction. It produces two photons of 511 keV emitted in opposite directions. Annihilation radiations are then imaged using a system dedicated to PET. This system operates on the principle of coincidence, i.e. the difference in arrival times of the photons of each pair of detected photons and by knowing that each annihilation produces two photons emitted in exactly opposite positions.

Our previous attempt to use cooperative coevolution was in SPECT [10]. It is based on the fly algorithm [9]. Each fly represents a point of the patient 3D space and it acts as a radioactive emitter. The final population of flies corresponds to the tracer density in the patient who is scanned, i.e. the reconstructed data. It uses a "marginal fitness" metrics based on the "leave-one-out cross-validation" method to evaluate the contribution of each fly as it will be explained in detail in Section 3.1. This metrics gives the contribution (positive or negative) of a given fly with respect to the whole population. In SPECT, the input data corresponds to raw 2D projections at successive angles around the patient that can be formated into a sinogram format. However, to speed up the reconstruction time and reduce the amount of memory needed by the algorithm, only 3% of the input data is used at a time by a fly during the reconstruction. Indeed, for each fly, only four orthogonal projections are simulated.

This SPECT reconstruction approach, based on artificial evolution, gave promising results. However, PET is considered to be the gold-standard tomographic technique in nuclear medicine due to its higher sensitivity. The section below shows how to adapt the fly algorithm more efficiently in this case, taking into account the specificity of PET data.

3 Reconstruction Method

3.1 Artificial Evolution Algorithm For PET

In [10], we showed that, when we were addressing the SPECT problem, if we defined the fitness of a fly as the consistency of the image pattern it generates, with the actual images, it gave an important bias to the algorithm with a tendency of the smaller objects to disappear. This is why we then introduced marginal evaluation, where the fitness of a given fly is not evaluated in itself, but as the (positive or negative) contribution to the likeness of the image produced by the complete population of flies, with the current image.

In other terms, to evaluate a given fly, we first evaluate the fitness of the whole population - the distance between the total illumination pattern created by all the flies, to the actual image - then evaluate the fitness of the same total population without the fly that is being evaluated, and calculate the difference:

$$\text{fitness}_{\text{m}}(i) = \text{fitness}\,(\mathit{population} - \{i\}) - \text{fitness}\,(\mathit{population}) \qquad (1)$$

with $\text{fitness}_{\text{m}}(i)$ the marginal fitness of a given fly, $\text{fitness}\,(population - \{i\})$ the fitness metrics of the population without the fly that is being evaluated, and $\text{fitness}\,(population)$ the fitness metrics of the whole population of flies.

This particular method to calculate fitnesses does not induce any extra computation load. Each time a new fly is created, a simulation is done in order to calculate its illumination pattern, which is kept in memory. Each time a fly is destroyed or created, the total illumination pattern is updated. When a fly has to be evaluated, the global fitness is readily calculated using the total illumination pattern, and the global fitness "minus one" is calculated the same way using the "total minus one" illumination pattern.

This fitness calculation method is then integrated into an evolution strategy scheme (see Figure 1). The population of flies is first initialised randomly. In the

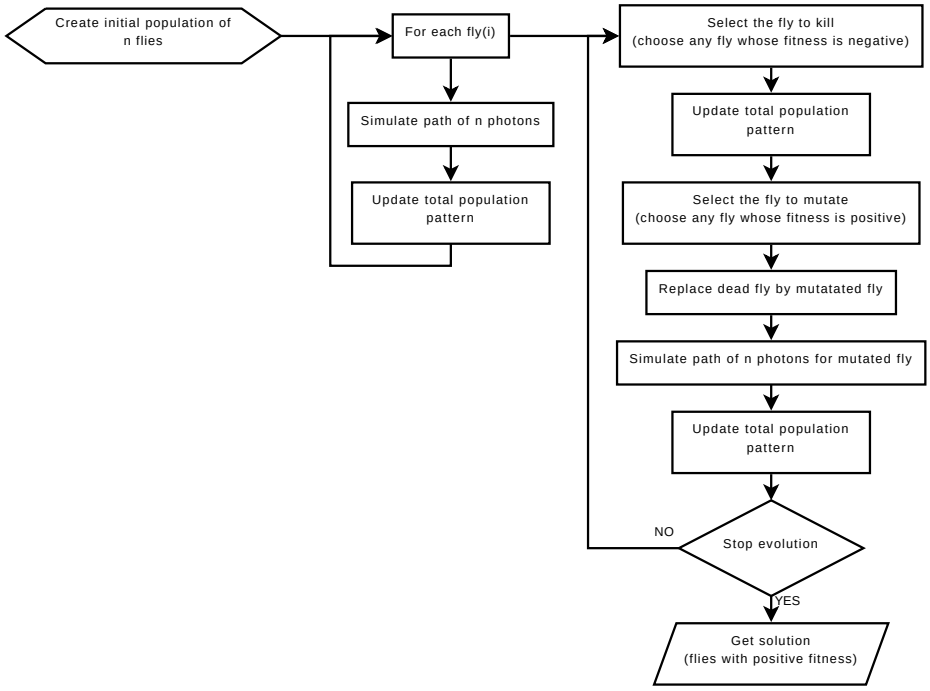

Fig. 1. Reconstruction algorithm.

test experiments shown in this paper, the flies are initialised inside a cylinder contained between the sensor crystals. In real applications, the actual shape of the body may be used. In the second part of the initialisation, in the case of SPECT, a fly produces an adjustable number of photons to compute its own image pattern. Once each pattern is computed, the sum of these patterns is stored as the population's pattern and the population's global fitness is calculated by comparing the pattern to the actual image. In the case of PET, each fly is pro-

ducing an adjustable number of annihilation events. The result of this simulation consists of a list of pairs of detector identification numbers that correspond to annihilations (see Section 3.3 for details). There begins the evolution loop. An interesting point is that our method to calculate the fitness delivers negative values for flies with a negative contribution and positive values otherwise. Therefore it was attempting to skip the classical selection step and use a fixed threshold - zero! - as the only selection criterion. Thus we built a steady state evolution strategy, where in order to choose the fly that has to be replaced, we draw flies randomly until a fly is found with a negative fitness. Then it is eliminated and replaced by the application of evolutionary operators to a parent fly chosen the same way but with a positive fitness.

3.2 Sinogram Mode

During the annihilation, two photons of 511 keV are emitted in opposite directions. Photons of a single pair are called coincidence photons. When two photons are detected within a predefined time window 2τ, the PET imaging system records which crystals have been activated, i.e. the position of the photons within the imaging system.

It is possible to convert the coincidence data into a sinogram format [13]. This is convenient as it enables the use of standard reconstruction methods that have been originally developed for CT or SPECT. Fig. 2 shows how this conversion can be achieved. When an annihilation event occurs, two photons are emitted in coincidence at 180 degrees. Two detectors are activated almost at the same time. The line between the activated detectors is called a "line of response" (LOR). To generate a sinogram, sampling is needed along:

- the horizontal axis of the sinogram that matches the minimum distance between a LOR and the centre point of the system (see distance r in Fig. 2),
- the vertical axis of the sinogram that matches the angle between a LOR and the horizontal plane of the system (see angle α between the LOR and the dash line in Fig. 2).

Then it is possible to use a reconstruction method that is similar to the one that we initially proposed for SPECT data. However, we saw that using sinograms in PET introduces drawbacks (such as sampling, difficulties to take advantages of physics and geometrical properties of the imaging system, memory usage, etc.) and that, therefore, a new approach dedicated to PET is required.

3.3 LOR Mode

It is possible to model the actual geometry of the imaging system to directly use the coincidence data without any conversion. In practice, PET imaging systems are made of blocks of collinear detectors [14]. These blocks are located circularly to constitute a cylinder. Each crystal is identified by a unique identification number. Note that several cylinders of blocks are used in a PET scanner.

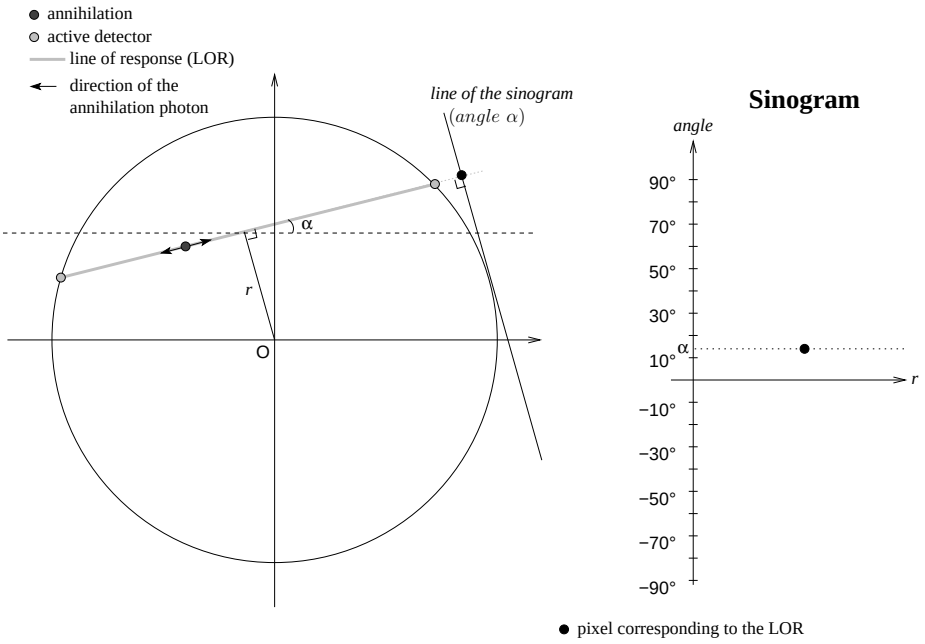

Fig. 2. Conversion from coincidence events to 2D sinograms.

Here, a fly acts as a positron that will emit random pairs of coincidence photons. The number of pairs per fly is a parameter that can be tuned. For each pair of photons, a direction is picked using uniformly distributed random points on the surface of a unit sphere. It gives the direction of the first photon of the pair, whilst the opposite vector gives the direction of the other photon. The fly's position and the photon's direction define a line. When this line intersects two crystals, a LOR is detected. Using efficient ray-tracing techniques (ray-tracing is widely documented in the literature, and a complete overview can be found in *3D Computer Graphics* by A. Watt [15]), it is possible to detect intersections. To speed up computations, the PET scanner is embedded into a bounding open cylinder. If one of the rays corresponding to a pair of photons does not intersect the bounding cylinder, then no LOR will be detected. In this case, intersections between the rays and the crystals are skipped. Fig. 3 shows a simplified PET system with simulated LORs.

To evaluate a fly's contribution, the concept of marginal fitness is used once again (see Eq. 1). The fitness metrics corresponds to a distance measurement between simulated data and the actual data given by the imaging system (note that data must be normalised). A LOR needs to be modelled using a pair of detector identification numbers. LORs cannot be efficiently accumulated in 2D images. Due to the fitness function, two lists are needed, one for the actual data, and one for the population data. The number of times a given LOR is encountered is stored in the corresponding record. Actual and simulated data

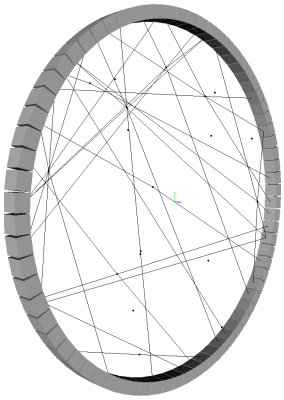

Fig. 3. Using a simplified PET system geometry.

are efficiently stored into indexed lists (the standard template library (STL) provides such containers [16]). The pair of identification numbers is used as the key of each record in the lists. It speeds up the memory access to records and reduces memory usage to its minimum. Indeed, empty records, when a pair of crystal identification numbers do not correspond to a LOR, are not stored. Also, each fly needs to store the LORs that it has generated. In this case, the fitness can be computed using a distance measurement between the lists. For efficiency reasons, we have chosen the City Block Distance metrics (sometimes called Manhattan Distance):

$$\mathrm{d}(LOR_r, LOR_s) = \sum |LOR_r(key).counter - LOR_s(key).counter| \quad (2)$$

with $\mathrm{d}(LOR_r, LOR_s)$ the city block distance between LOR_r and LOR_s, the set of LORs for the real data and the simulated data respectively, and *counter* is the number of times that a given key appears in the LOR set. To compute Eq. 1, LOR_s corresponds either to the set of LORs of the whole population of flies or the set of LORs of the population without the fly that is being evaluated.

4 Results and Validation

This section presents the results obtained using synthetic data to validate the usefulness and accuracy of our novel PET reconstruction approach. First, we compare images reconstructed from sinograms using our algorithm with reference images computed with an OS-EM implementation. Then, we evaluate images reconstructed from LOR data with respect to theoretical values.

4.1 Sinogram Mode

Let us consider the set up presented in Fig. 4. It is made of two spheres whose

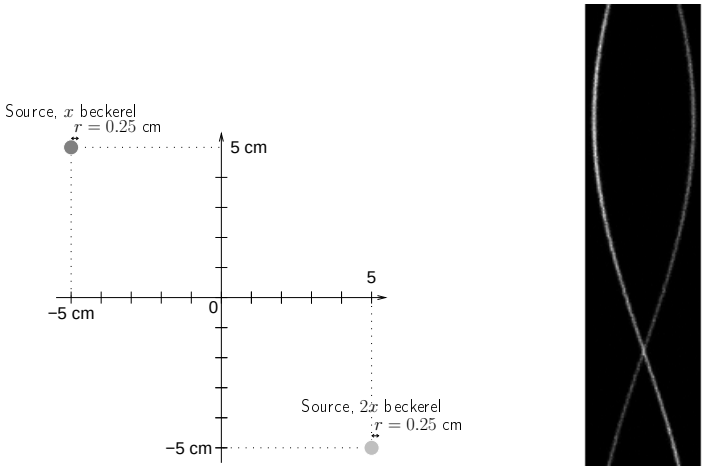

(a) Set up. (b) Sinogram.

Fig. 4. Test sinogram.

radius is 2.5 mm. The radioactivity of one of them is twice as great as the other one's activity.

Fig. 5 shows examples of tomographic slices reconstructed using our evolutionary method and the OS-EM algorithm. Method 1 consists in incrementing

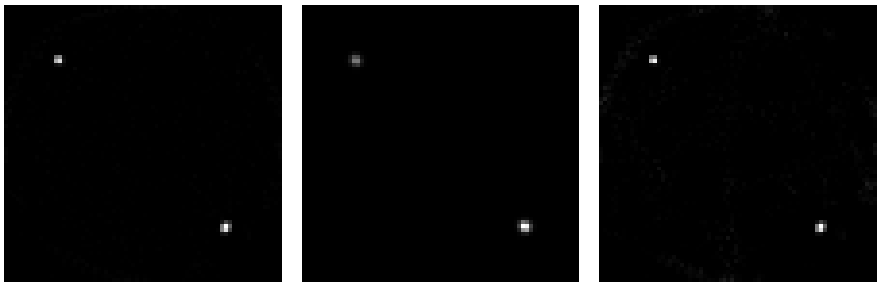

(a) Method 1. (b) OS-EM (c) Method 2.

Fig. 5. Tomographic slices reconstructed using Fig. 4(b).

the voxel value of the reconstructed volume for each fly that lies in that voxel. Method 2 consists in accumulating the marginal fitness of each fly whose fitness is positive and that lies in that voxel. The final volume data is then normalised between 0 and 1. This normalisation step is needed to compare results with the volume that has been produced using the OS-EM algorithm. Reconstructed volumes appear to be visually similar to the reference volume.

To further compare the results, profiles are extracted at the centre of each bright area in Fig. 5. Fig. 6 shows that these profiles are relatively close. In

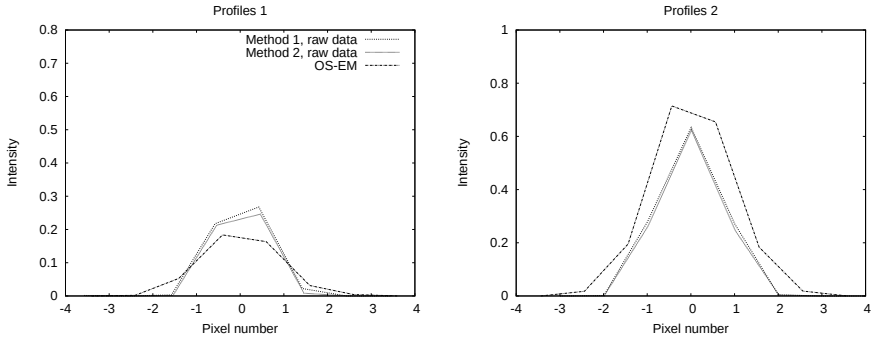

(a) Upper left bright area. (b) Lower right bright area.

Fig. 6. Profiles extracted from Fig. 5.

particular, the difference of intensity between the two bright areas is preserved in the reconstructed slices.

4.2 LOR Mode

Test 1 Nine spheres with various radius and radioactivity are simulated in this test. Fig. 7 shows both the reconstructed and real data. Reconstructed volumes

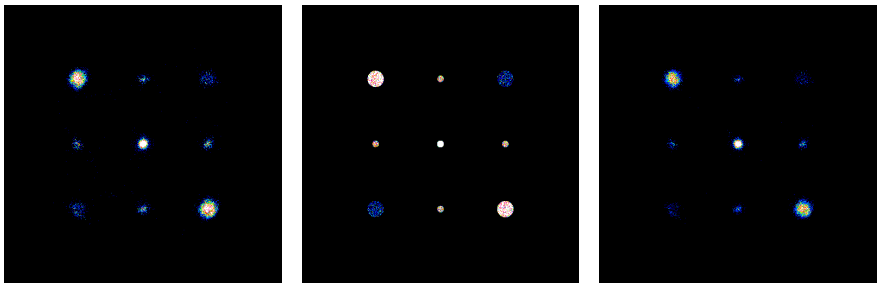

(a) Method 1. (b) Real data. (c) Method 2.

Fig. 7. Tomographic slices.

appear to be visually similar to the reference volume.

Once again, to further compare the results, profiles are extracted at the centre of each bright area in Fig. 7 (note that a mean filter is used to reduce

the noise level). Fig. 8 shows that these profiles are relatively close. The profiles

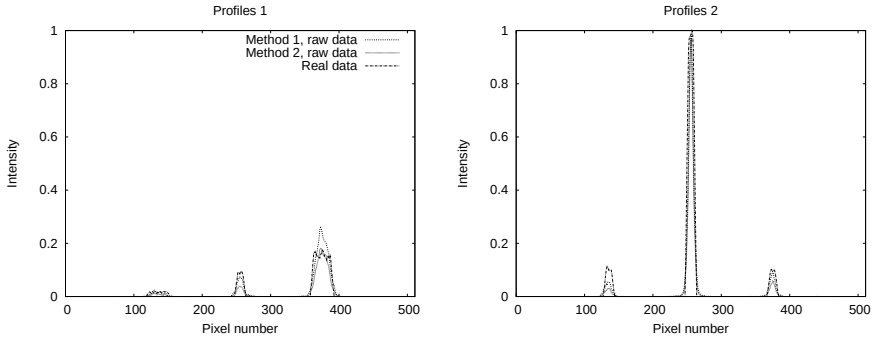

(a) Lower bright areas. (b) Middle bright areas.

Fig. 8. Profiles extracted from Fig. 7.

of the upper bright areas will be symmetrically similar to those of the lower areas. The radius of each sphere accurately matches the corresponding radius in the reference volume. Also, the difference of radioactivity is preserved in the reconstructed slices.

Test 2 Two cubes are simulated in this test. Fig. 9 shows the raw data after tomographic reconstruction and the real data. Likewise, reconstructed volumes

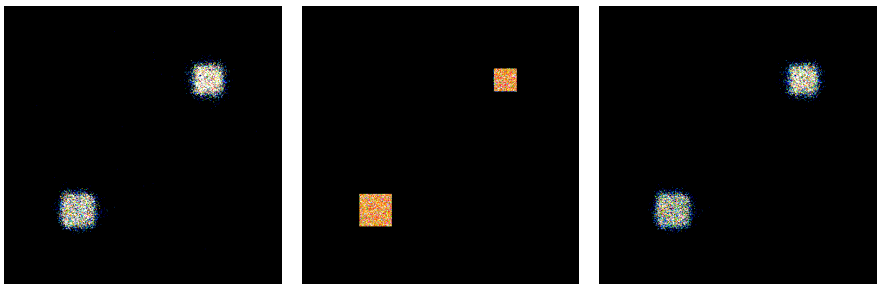

(a) Method 1. (b) Real data. (c) Method 2.

Fig. 9. Tomographic slices.

appear to be visually similar to the reference volume. Using the same method, profiles are extracted at the centre of each bright area. Fig. 10 shows that the cube lengths accurately match the real values.

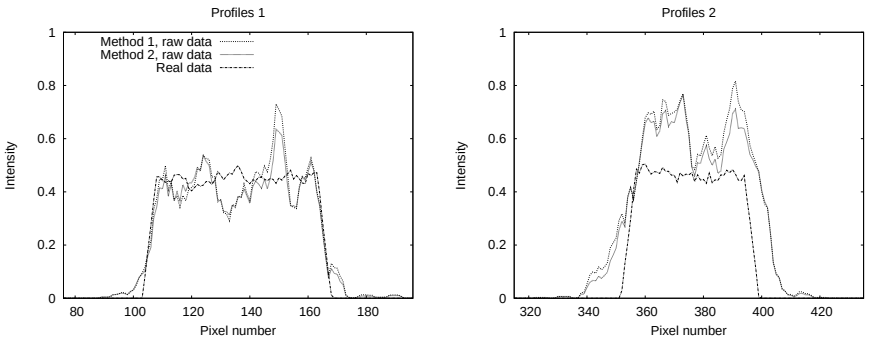

(a) Lower left bright area. (b) Upper right bright area.

Fig. 10. Profiles extracted from Fig. 9.

5 Discussion and Conclusion

In this paper, we show that Evolutionary Computation is a promising technique to solve the usually computationally expensive problem of reconstructing 3D images from PET data. Whilst it is possible to use sinograms in PET, this option is not acceptable. Instead, a simplified geometrical model of PET scanner is used to simulate annihilation events. To date, the photons' trajectory is simulated without interaction with matter. This approach is closer to reality and it gives promising results on synthetic data. Also, more realistic physics simulations could be added to correct Compton scattering.

Another point we have raised is that when using "marginal evaluation", an individual's fitness is not calculated in an absolute manner, but as the positive or negative value of the contribution of this individual to the performance of the complete population. A consequence is that the relatively costly step of selection may be skipped and the evolutionary algorithm be simplified. In addition, in some cases this may even result in a stopping criterion, if at some stage all the individuals have got a positive fitness value, which means they are all contributing positively to the reconstruction. This should be applicable into other areas of evolutionary computation and coevolution, not necessarily restricted to medical imaging, whenever the marginal fitness paradigm is used.

List of Acronyms

CT	computed tomography
LOR	line of response
ML-EM	maximum-likelihood expectation-maximization
OS-EM	ordered subset expectation-maximization
PET	positron emission tomography
SPECT	single-photon emission computed tomography
STL	standard template library

Acknowledgements

This work has been partially funded by *Agence Nationale de la Recherche (ANR)*.

References

1. Shepp, L.A., Vardi, Y.: Maximum likelihood reconstruction for emission tomography. IEEE Transactions on Medical Imaging **1**(2) (1982) 113–122
2. Hudson, H.M., Larkin, R.S.: Accelerated image reconstruction using ordered subsets of projection data. IEEE Transactions on Medical Imaging **13**(4) (1994) 601–609
3. Lewitt, R.M., Matej, S.: Overview of methods for image reconstruction from projections in emission computed tomography. Proceedings of IEEE **91**(10) (2003) 1588–1611
4. Olague, G., Cagnoni, S., Lutton, E.: Introduction to the special issue on evolutionary computer vision and image understanding. Pattern Recognition Letters **27**(11) (2006) 1161–1163
5. Pea-Reyes, C., Sipper, M.: Evolutionary computation in medicine: an overview. Artificial Intelligence in Medicine **19**(1) (2000) 1–23
6. Bosman, P.A.N., Alderliesten, T.: Evolutionary algorithms for medical simulations: a case study in minimally-invasive vascular interventions. In: Proceedings of the 2005 workshops on Genetic and evolutionary computation (GECCO '05). (2005) 125–132
7. Cagnoni, S., Dobrzeniecki, A.B., Poli, R., Yanch, J.C.: Genetic algorithm-based interactive segmentation of 3d medical images. Image and Vision Computing **17**(12) (1999) 881–895
8. Völk, K., Miller, J.F., Smith, S.L.: Multiple network CGP for the classification of mammograms. In: EvoWorkshops. Volume 5484 of Lecture Notes in Computer Science., Springer (2009) 405–413
9. Louchet, J.: Stereo analysis using individual evolution strategy. In: Proceedings of the International Conference on Pattern Recognition (ICPR '00). (2000) 1908
10. Bousquet, A., Louchet, J., Rocchisani, J.M.: Fully three-dimensional tomographic evolutionary reconstruction in nuclear medicine. In: Artificial Evolution (EA '07). Volume 4926 of Lecture Notes in Computer Science. (2007) 231–242
11. Badawi, R.D.: Nuclear medicine. Physics Education **36**(6) (2001) 452–459
12. Michael, G.: X-ray computed tomography. Physics Education **36**(6) (2001) 442–451
13. Fahey, F.H.: Data acquisition in PET imaging. Journal of Nuclear Medicine Technology **30**(2) (2002) 39–49
14. Townsend, D.W.: Physical principles and technology of clinical PET imaging. Annals of the Academy of Medicine **33**(2) (2004) 133–145
15. Watt, A.: 3D Computer Graphics. 3rd edn. Addison-Wesley (2000)
16. Silicon Graphics, Inc.: Standard template library programmer's guide. Available at http://www.sgi.com/tech/stl/ (accessed 6 May 2009).